



# A shifting pattern of tropical cyclone induced high river discharges in the Greater Mekong Region, 1970-2019

Stephen E. Darby<sup>1</sup>, Ivan D. Haigh<sup>2</sup>; Melissa Wood<sup>2,6</sup>; Bui Duong<sup>3,4</sup>, Tien Le Thuy Du<sup>4</sup>, Thao Phuong Bui<sup>1,3</sup>, Justin Sheffield<sup>1</sup>, Hal Voepel<sup>1</sup>, Joël J.-M. Hirschi<sup>5</sup>

<sup>1</sup> School of Geography and Environmental Science, University of Southampton, Highfield, Southampton, UK

<sup>2</sup> School of Ocean and Earth Science, University of Southampton, Waterfront Campus, European Way, Southampton, UK

<sup>3</sup> Science, Technology and International cooperation Department, National Center for Water Resources Planning and Investigation (NAWAPI), Ministry of Natural Resource and Environment (MONRE), Hanoi, Vietnam

<sup>4</sup> Department of Civil and Environmental Engineering, University of Houston, USA

<sup>5</sup> National Oceanography Centre, European Way, Southampton, UK

<sup>6</sup> National Oceanography Centre, Joseph Proudman Building, Liverpool, UK

Correspondence to: Stephen E. Darby (s.e.darby@soton.ac.uk)

## Abstract

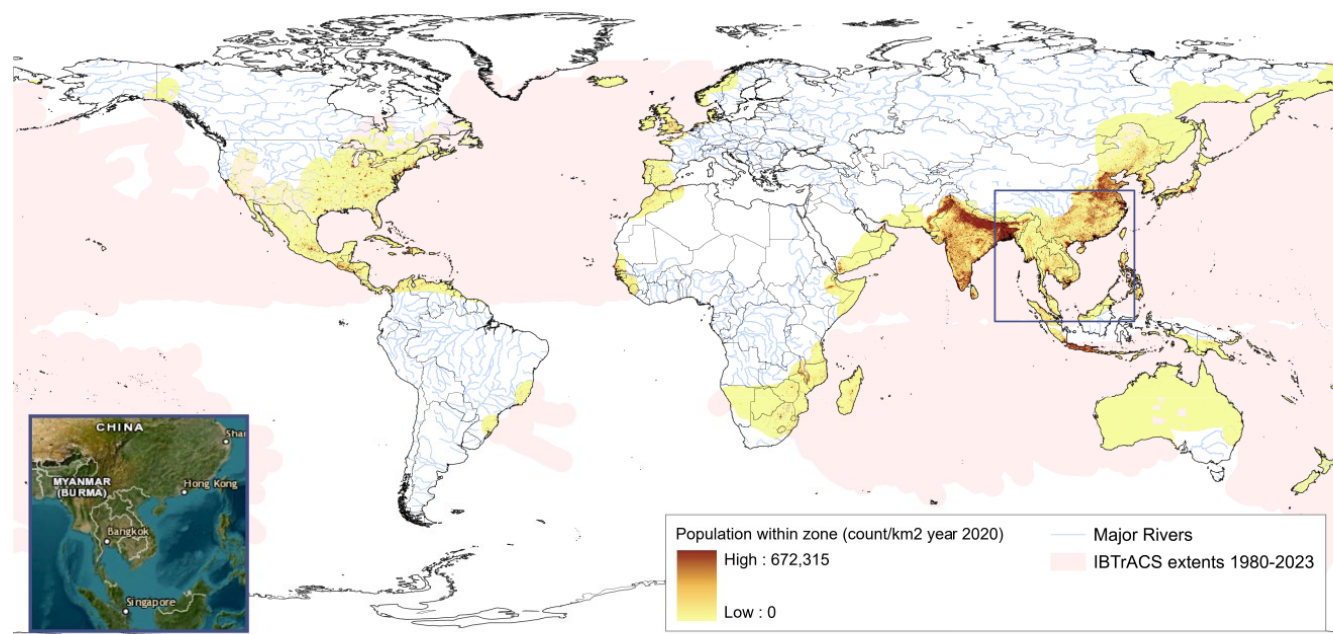
On average flood events impact over 100 million people globally every year, and because of demographic changes and economic development in flood-prone areas, as well as climate change, the population exposed to flood risk is expected to double by 2050. Under anthropogenic climate change it is expected that flood events previously considered extreme will be occurring with more frequency, due to changing patterns of precipitation in a warming climate. It is, therefore, critically important to better understand how extreme weather events generate high river flows in exposed regions. Here we look specifically at the influence of precipitation from tropical cyclone (TC) activity on high river flows within one such exposed region: a 1.2 million km<sup>2</sup> area of southeast Asia encompassing the entirety of the Mekong and Red River catchments, plus 13 smaller catchments along the coastal fringe of Vietnam (collectively referred to here as the Greater Mekong region, or GMR). We use a hydrological model (GM-HYPE) with ERA5 precipitation data to simulate streamflows over the last 50 years (1970-2019) with, and without, TC-linked precipitation. Our results demonstrate that TC-linked precipitation around the GMR generate notable increases in high (95<sup>th</sup> percentile) streamflows, and this is most notable in the steep sub-catchments draining to Vietnam's northern coastline. These locations are more exposed to TC activity, and we determine that the elevated soil moisture levels there from monsoonal precipitation, prior to the typhoon season, are an exacerbating factor. Furthermore, trend analysis also shows that shifts in the spatial locations of TC-induced high river flows have been occurring since the 1970s: while statistically significant increases in TC-induced high river discharges are evident in localised regions of the GMR including the highlands of Laos and the Mekong's delta region, declines in TC-induced high river discharges are much more widespread, with notable declines in the headwater and middle reaches of the Red and Mekong Rivers. Our findings on the changing pattern of high river flows in recent decades, in a region highly exposed to TCs, will be of great interest to strategic planners and flood managers. We conclude with a discussion on the impact of global climate model precipitation projections for this region, contrasting past/present (1980-2014), and future (2016-2050), GM-HYPE model results.



## 35 1 Introduction

Flooding sustains a range of vital ecosystem services, but also has devastating impacts on people, infrastructure and the environment (Hirabayashi et al., 2013). Flood events already impact >100 million people each year (Di Baldassarre et al., 2013), but flood hazard is projected to increase in the future, in part driven by the increasing frequency of extreme precipitation events anticipated under greenhouse warming (Arnell and Gosling 2013). For example, 21<sup>st</sup> century climate change scenarios project further increases in the frequency and intensity of extreme hydro-climatological events (Polade et al., 2017) that are expected to generate substantial increases in peak river discharges across the globe (Hirabayashi et al., 2013; IPCC 2018). Flood risk, the product of flood hazard and the vulnerability and exposure of people and assets, is also increasing because of demographic changes and economic development in flood-prone areas (Kundzewicz et al., 2014; Jongman et al., 2015; Devitt et al., 2023; Rentschler et al., 2023). This means that over large swathes of the Earth, flood risk is set to double by 2050, substantially increasing the 1.8 billion people already living in areas where the annual probability of flooding exceeds the 1 in 100-year flood event, the defence standard often adopted as the baseline by water agencies (Rentschler et al., 2022).

Anthropogenically-induced increases in the extreme precipitation events that drive flooding are caused in large part by the increased capacity of a warmer atmosphere to absorb moisture evaporated from the oceans. However, in some regions of the world extreme precipitation events are commonly associated with the passage of tropical cyclones (TCs). Where these storms propagate inland, the heavy rainfall can lead to substantial flooding (Murakami et al., 2013), as exemplified by major flood catastrophes including the 2008 Cyclone Nargis (Myanmar), the 2013 Cyclone Haiyan (Philippines), and the 2024 Hurricane Helene (USA) and Typhoon Yagi (Vietnam). In fact, we estimate that around 65% of the global population currently lives in regions that have been affected by tropical and extra-tropical cyclones (Fig. 1: year 2020 populations within the bounds of historical Tropical- and Extra-Tropical-Cyclone tracks, with a 300km buffer around cyclone epicentres, as defined by IBTrACS - Knapp et al., 2010). Figure 1 shows that large numbers of people living in East and southeast Asia, the Bay of Bengal, and the Gulf of Mexico are particularly at risk. Within such regions, it is disproportionately older people and the socioeconomically deprived that are regularly exposed to TC hazards (Jing et al., 2024).



60 **Figure 1 – Extent of tropical and extra-tropical cyclone storm tracks 1980-2023 from IBTrACS (Knapp et al., 2010): a 300km buffer**  
**around storm epicentres is shaded red, from cyclogenesis to dissipation. The yellow areas highlight smaller populations historically**  
**exposed, with the darkest brown shading indicating the greatest population densities (year 2020, from WorldPop, 2023). Inset: The**  
**Greater Mekong Region study area (credits: Esri 2025 and Earthstar Geographics 2025).**

In the future, while the warmer temperatures associated with anthropogenic climate change projected by most climate  
65 models might not lead to overall increases in the total numbers of TCs, a larger fraction of them are anticipated to grow to the  
strongest categories (Saffir-Simpson category 3, 4, 5) and the precipitation intensity associated with TCs is expected to  
increase. Shifts in the position of TC tracks towards the poles are also expected (Knutson et al., 2010; Murakami et al., 2013;  
Roberts et al., 2020; Bloemendaal et al., 2022). This suggests that the flood damages caused by TCs will likely be altered in  
the future, driving an increased need for risk adaptation and resilience to these types of extreme weather events in those regions  
70 that will be disproportionately affected (Gupta et al., 2019).

For these reasons, understanding the effect of climate change on TCs – including their frequency, intensity, location and  
their associated natural and societal impacts – remains a priority. Previous research has tended to focus on changes in TC  
characteristics such as frequency, intensity and track geography (Knutson et al., 2010; Murakami et al., 2013; Gupta et al.,  
2019; Roberts et al., 2020; Bloemendaal et al., 2022), while some studies have also explored the effects of these changes on  
75 precipitation distributions over land (Englehart and Douglas 2001; Franco-Diaz et al., 2019; Ali et al., 2023). However, there  
have been fewer studies that explore the implications for changes in flood hydrology, and this is especially notable for regions  
such as southeast Asia that have dense populations exposed to TCs. Sun et al., 2021, and Macalalad et al., 2021 explored this  
theme, showing that precipitation from landfalling TCs will induce and augment river flooding within catchments in the Mid-  
Atlantic USA and the Philippines. Darby et al., (2016) modelled 25-years of river flows within the Mekong River catchment,



80 finding that intense precipitation linked to TCs (at annual timescales) is responsible for a substantial proportion of annual surface runoff in the catchment.

To address this research gap, here we quantify the influence of TC activity on high river flows within a 1.2 million km<sup>2</sup> area of southeast Asia (5° N to 35° N and 90° E to 115° E) encompassing the Mekong and Red River catchments, plus 13 smaller catchments located along the coastal fringe of Vietnam. In 2020, this Greater Mekong Region (GMR) supported a population  
85 of over 160 million people (Ali et al., 2023). To explore the implications of TC-activity on flood hydrology in the GMR, we have two specific objectives:

- O1. Quantify the influence of TCs on high streamflow characteristics, across the GMR, by using a hydrologic model - that we force with, and without, historic TC precipitation data; and
- O2. Identify the factors driving altered streamflows by using stepwise linear regression to identify the relationships between  
90 streamflow, excess precipitation, soil moisture, and catchment attributes such as slope.

## 2 Methods

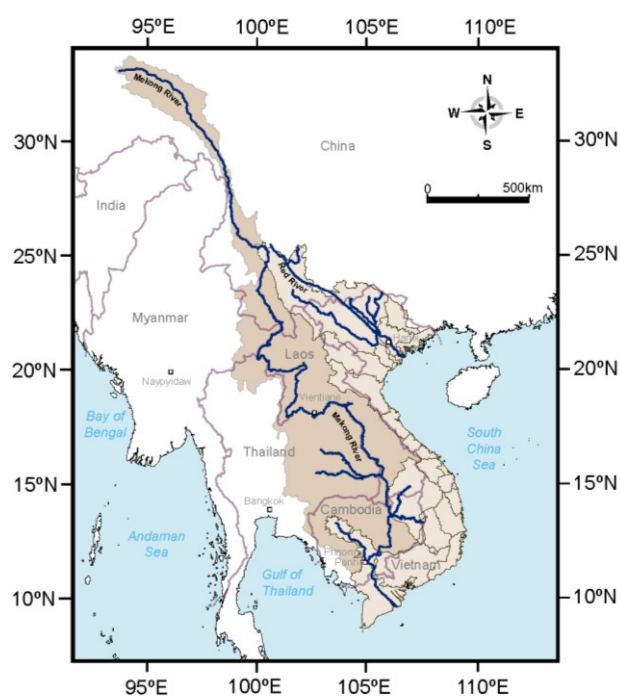


**Figure 2 – GM-HYPE model domain, showing extents of the Greater Mekong Region (GMR: shaded brown), and river sub-catchments outlined. The Mekong and Red Rivers are also indicated.**

To address objective 1, we utilise a Hydrological Predictions for the Environment (HYPER) semi-distributed hydrological model, created to simulate the flood hydrology of the GMR's major sub-catchments (shaded brown in Fig. 2), named 'GM-HYPE' v1.4 (Lindström et al., 2010; Du et al., 2022). GM-HYPE v1.4, covers our 1.2 million km<sup>2</sup> study area encompassing 13 major river basins of Vietnam, Laos, and Cambodia, and parts of China, Thailand, and Myanmar. The GM-HYPE models calculate river discharge timeseries by dividing the GMR into 1,230 sub-catchments, incorporating the flows around operating reservoirs and dams (constructed up to the year 2020).

A detailed description of the model's set up, and validation results, are given in Supplementary Material 1. In summary, prior validation studies have indicated that GM-HYPE produces robust simulations of river flows in the GMR. When forced with ERA5 input climate data, comparison of model outputs with observations at ~30 gauges internal to the GMR model domain shows that the model delivers a Kling-Gupta Efficiency of 0.60



and 0.72, and a Pearson's correlation coefficient of 0.78 and 0.84, for the periods 1991-2001 and 2016-2019, respectively.

For this study, GM-HYPE simulations were forced with ERA5 reanalysis total precipitation data downloaded from the Copernicus climate data store (<https://cds.climate.copernicus.eu>; Hersbach et al., 2020), for the period 1970-2019. ERA5 data has been well validated against Global Climate Models (e.g. Gebrechorkos et al., 2023). A full 50-years of data was selected for long-term change assessment. To isolate TC -linked precipitation from all other sources of precipitation for this region, we created two separate GM-HYPE models to simulate sub-catchment scale discharges and used differencing. The first model (Model A), is the GMR baseline model, forced with both monsoon and TC-linked precipitation. A second model (Model B) reproduces this baseline model but with TC-induced precipitation clipped out (the TC-induced precipitation being defined as any precipitation within a 500km radius of the TC epicentre, following the approach of Darby et al. 2016; Rodgers et al., 2000; and Englehart and Douglas 2001), without replacement, in the precipitation forcing file. This 500 km radius is conservative compared to previous studies. To identify the epicentre and track of the TCs over the study period, we extracted data from the IBTrACS database (Knapp et al., 2010). We note that both ERA5 and IBTrACS database are generally considered less reliable before the advent of satellite era (beginning in the 1980s) compared to those from later periods (Kossin et al., 2020).

From the models' outputs, we calculated low (5<sup>th</sup> percentile), mean, and high (95<sup>th</sup> percentile) stream flow metrics for each of the 1,230 sub-catchments outflow points. TC-linked streamflow excess, at every sub-catchment, was thus calculated as the difference between the Model A and Model B simulated discharges. The 1970-2019 high streamflow results are presented in the results section and discussed in section 4. For clarity, we also report mean streamflow results in Supplementary Material 2 (Fig. S2.1).

To address objective 2, for each sub-catchment in the GM-HYPE domain, we used a Mann Kendall regression analysis to look for strength and direction of trends in the GM-HYPE models A and B output streamflow timeseries data. Subsequently we used a linear regression model to explore the difference between the means of key model variables, to determine which could be affecting excess high streamflows. We selected three independent variables: sub-catchment (1) excess precipitation, (2) excess soil moisture (both relative to the no-TC precipitation model), and (3) sub-catchment slope.

Lastly, as a discussion point, we considered how future extreme precipitation events may impact high streamflows in the GMR. We extracted local precipitation fields, combining monsoon and TC events, from a high-resolution SSP5-8.5 global climate model (GCM) simulating the period 1950 to 2050 (Roberts et al., 2019). Splitting the data, we created a new pair of GM-HYPE models – one for a past/present (1980 to 2014, Model C), and one for a future (2016 to 2050, Model D) climate. From the outputs of Models C and D, we again calculated the 1980-2014 and 2016-2050 mean, and high, streamflows. The changing profile of high streamflows in the GMR due to global warming are presented in the results section (whereas mean streamflow results are presented in Supplementary Materials 5).



### 3 Results

First we present the results from differencing Model A and B high (95<sup>th</sup> percentile) river discharges for the recent past (1970-2019), in Fig 3. These figures show that the greatest excess of high river discharge is located in the lower Mekong River channel and delta, where high flows increase by up to an additional 3,500 m<sup>3</sup>s<sup>-1</sup> (Fig. 3c). However, proportionally this increase represents only a <10% relative change. Instead, in terms of percentage changes, it is the smaller, steeper sub-catchments in Vietnam's coastal north (south of the Red River delta, such as the Lam River catchment), that are more intensely affected in terms of increased high flows, with the 95<sup>th</sup> percentile discharges in these areas increasing by up to 50%, as shown in Fig. 3d. Inland, tributaries feeding the Mekong River (e.g., the Mun/Chi Rivers, Thailand), and sub-catchments in Khammouane/Savannakhet provinces (Laos), also show substantial (up to 35%) relative increases in high streamflows. Mean streamflow results are provided in Supplementary Materials 2, and these show similar patterns.

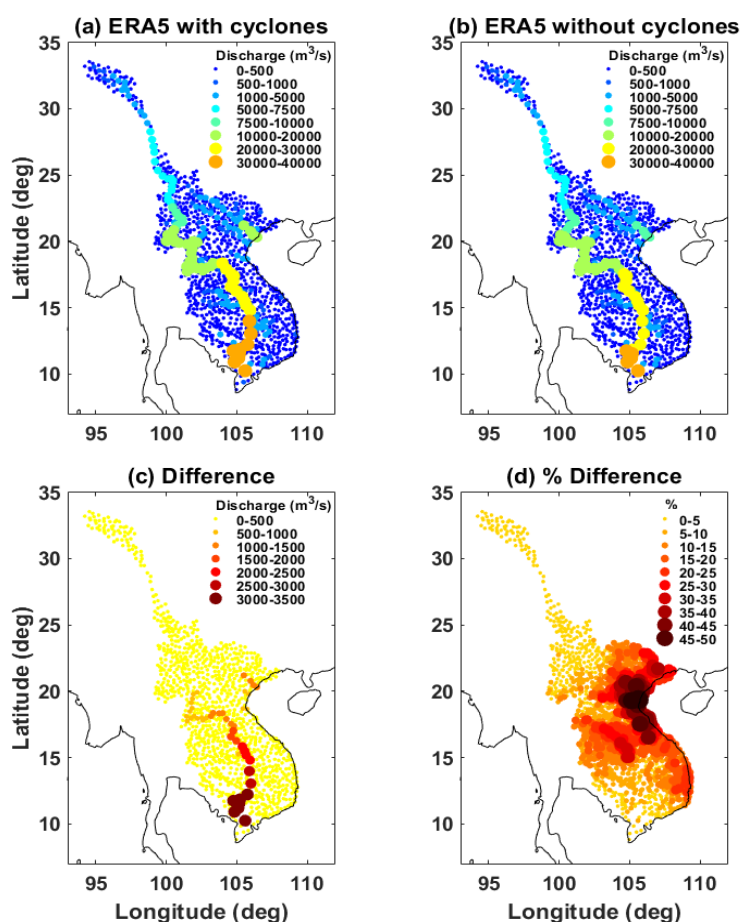


Figure 3 – HYPE's 95<sup>th</sup> percentile river discharge per sub-catchment [units m<sup>3</sup>s<sup>-1</sup>], for the models which a) include TC-derived rainfall, b) exclude TC-derived rainfall, c) the difference between (a) and (b) in m<sup>3</sup>s<sup>-1</sup>, and d) the percentage difference between (a) and (b).





To assess trends in the TC-precipitation-linked excess streamflows identified during our period of record, we calculated Mann-Kendall Sen slope (S) (Mann 1945; Burkey 2021) which indicates strength of trends in timeseries data. Figure 4 presents the Sen slope results so-derived for high flows: with (Fig. 4a); and without (Fig. 4b); TC-linked precipitation. Figure 4(c) shows the difference, thereby highlighting the impact that the TC-linked precipitation makes. With, or without, TC-linked precipitation, the overall trend is negative ( $\geq -200 \text{ m}^3\text{s}^{-1}$  per year) for the majority of GMR sub-catchments. The equivalent plot for mean flows is given in Supplementary Material 4, Fig. S4.1.

An 'x', in Figure 4(a) and 4(b), marks locations where the computed trend is statistically significant ( $\alpha < 0.05$ ); such reaches are geographically located mainly in the elevated headwaters and main branches of both the major Red and Mekong Rivers. Isolated pockets of positive trend in high river discharge are also evident, such as: (1) in the Mekong tributaries within the Laos highlands; close to Khong Chiam (at  $\sim 16^\circ \text{ N}$ ); (2) in select Red River sub-catchments; (3) around the Ca River headwaters; (4) along the Mekong River in China; and (5) in the Cambodian and Vietnamese Mekong delta. However, these positive trends are statistically significant only in the Laos highlands and Mekong delta region.

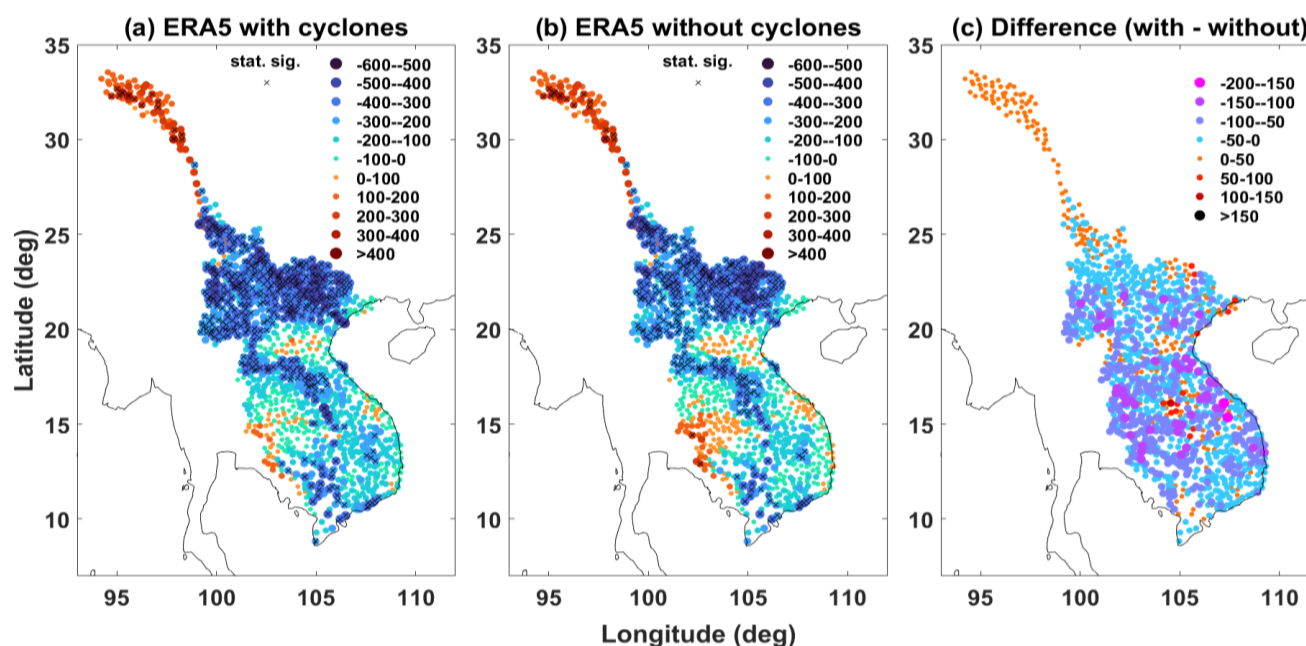


**Figure 4 – Mann Kendall ‘S’ (Sen slope) statistic, showing magnitude or strength of long-term trend - calculated on 95<sup>th</sup> percentile river flows at each sub-catchment. Sub-catchments with an ‘x’ have statistical significance at  $\alpha=0.05$ . Comparing (a) ERA5 precipitation including TCs; with (b) ERA5 precipitation without TCs. (c) is the direction of the trend.**

To identify the potential factors driving the excess high streamflows, we evaluated the role of: (1) catchment excess precipitation; (2) catchment excess soil moisture; and (3) catchment slope using Ordinary Least Squares (OLS) regression. Modelled data were moderately to highly right skewed, which was log10 transformed to correct skew, thus setting up analysis of a power law model. Table 1 shows the only significant term, of these three, contributing to excess high stream flow is excess



soil moisture, which has an explained variation of 67% in the log-linearized OLS model. Inference of the final power law model  $Q = 10^{-3.441} ESM^{1.298}$  is that, on average, for every 1% mm increase in excess soil moisture there is a  $\sim 1.3\%$   $m^3s^{-1}$  increase in mean excess high stream flow. We did not examine interaction effects between the independent variables. Details of this regression analysis and the relationships between modelled outputs are provided within Supplementary Material 5.

**Table 1 – Results for OLS regression of a log-linearized power law model, where all variables were  $\log_{10}$  transformed. Three covariates were included in the model under the Term heading. Table also shows units, parameter estimates and evaluations.**

Term	units	Estimate	Standard Error	Statistic	p-Value
Intercept	-	-3.441	0.046	-74.296	<0.001
Excess precipitation	mm	-0.021	0.042	-0.503	0.615
Excess soil moisture	mm	1.298	0.028	46.180	<0.001
Mean sub-catchment slope	m/m	-0.006	0.025	-0.243	0.808

## 4 Discussion

Our results indicate that it is the coastal sub-catchments of Vietnam that have been most exposed to TC-linked precipitation activity during the 1970-2019 study period. Around the Black/Red River deltas, and further south in the smaller adjacent coastal sub-catchments around the Gianh, Song Ma, and Lam (Song Ca) Rivers in Vietnam, precipitation from TCs can increase high river discharges by up to an additional 50% as compared to discharges generated in the absence of TCs. Our results also indicate that the other key factor driving excess stream flow is excess soil saturation. Such excess soil saturation evidently arises due to wetting in the monsoonal months (May to September) immediately preceding the cyclone season (June to November), and because of wetting by the precipitation delivered by TCs themselves.

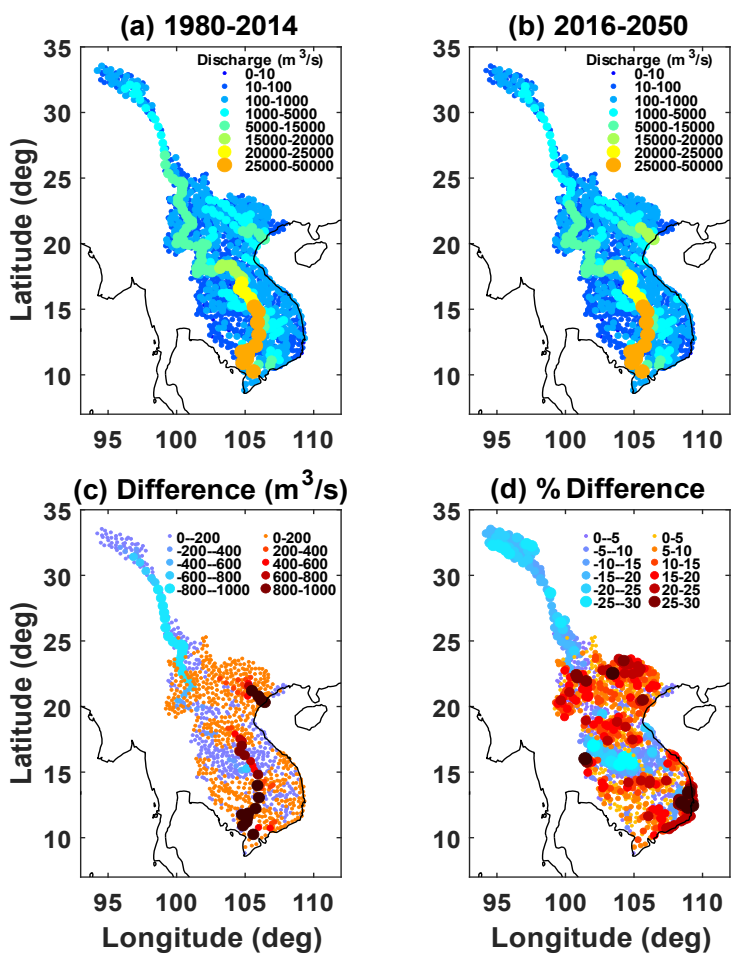
GCMs predict that in the coming decades the world will see elevated air temperatures, warmer seas, and inconstancy in the El-Niño Southern Oscillation (ENSO). In the Western North Pacific there are projected to be fewer low category TCs and a shift towards more intense cyclones (Knutson et al., 2015; Ali et al., 2023). Hence for the GMR, before the end of the century, we may see an increase in the intensity, pattern, and distribution of TC-linked precipitation together with changes to seasonal monsoons (Maher et al., 2023). If changing climatology alters the timing or duration of the regional monsoon seasons, as projected by GCMs, this has important implications for the GMR. Sub-catchments exposed to this new dynamic, of changed monsoon behaviour and more intense TC activity, need to prepare for the potential for new excesses in high streamflows over the coming decades.

To consider future high streamflows in the GMR, we compared past/present (1980-2014, Model C), and future (2016-2050, Model D), GCM-forced model results. We cannot reproduce the prior analysis for a past/present period (i.e. Model A versus Model B) because individual TC-tracks in the GCM-forced model input data cannot be isolated and identified, hence our future climate results include not only effects from TCs, but other climatological changes too. Our GCM-forced model results do, nonetheless, indicate that future high streamflows tend to increase relative to the past/present baseline, by approximately 300





210  $\text{m}^3\text{s}^{-1}$  to  $500 \text{ m}^3\text{s}^{-1}$ , across the majority of the GMR, but with increases of up to  $1,000 \text{ m}^3\text{s}^{-1}$  in both the main Mekong and Red Rivers (Fig. 5c). However, when expressed as a proportional change, hotspots of future change are especially evident in the upland headwaters of the Mekong and Red Rivers, and around Quy Nhon/Nha Trang in coastal central/southern Vietnam, which are projected to experience up to a 30% increase in high river discharges by 2050, relative to the 1980-2014 baseline (Fig. 5d). Whether driven by changes in future TC climatology, or other factors, these increases represent a substantial uplift in high river flows in those parts of the GMR that are already strongly susceptible to river flooding as a result of the passage of severe tropical storms. The equivalent mean streamflow statistical significance results are provided in Supplementary Material 6 (Fig. S6.1).



215 **Figure 5 – HYPE’s 95<sup>th</sup> percentile river discharge per sub-catchment (units  $\text{m}^3\text{s}^{-1}$ ), for the models with a) global climate model 1980-2014; b) global climate model 2016-2050 ; c) the discharge difference between them; and d) the % difference between them.**



## 5 Conclusion

Our analysis of ERA5-forced HYPE models of the Greater Mekong Region between 1970-2019, shows that high (95<sup>th</sup> percentile), and mean, river discharges are strongly responsive to TC-linked precipitation in certain regions of the model domain. Specifically, for the smaller coastal watersheds just south of the Red River delta, a region highly exposed to TCs, high streamflows associated with TCs are greater than - by as much as 50% - the high river discharges generated in the absence of TCs. Our study also shows that this augmentation of high river discharges is driven primarily by antecedent soil moisture conditions, with TC-induced precipitation especially effective in generating runoff when TCs cross over a landscape pre-wetted by the monsoon rains.

However, our study also reveals that during 1970-2019 there have been statistically significant declines in high TC-augmented streamflows across large parts of the GMR, including notably in the headwater regions and middle reaches of the Red and Mekong River basins. In contrast, statistically significant increases in high river discharges generated by TCs are evident in only two specific areas of the GMR, namely the highlands of Laos and the Mekong delta. This suggests that historical shifts in the pattern of TC tracks inland, alongside their changing intensity and frequency of occurrence, has led to changes in the geography of high streamflows generated by TCs during the last 5 decades.

Finally, we considered the question of how TCs and their role in generating high river flows might change in the future. Using projections from a global climate model to explore temporal trends in future high streamflows, up to the year 2050, we found that increases in high river discharges (that include all precipitation sources, not just rainfall from TCs) are projected in many Vietnamese coastal sub-catchments, especially between Quy Nhon and Ha Trang.

Our findings will be of interest to city planners, flood specialists, and river catchment managers throughout the GMR to help understand the nature of contemporary flood hazard and to consider how to future proof flood defences.

## 6 Acknowledgements

We would like to express our gratitude to the Water Resources Monitoring Department at NAWAPI, where various prior works with national and international partners over multiple years on the regional HYPE modelling platform, and extensive in situ data collection, made this study possible.

## 7 Funding

This study was supported by the Vietnam National Foundation for Science and Technology Development (105.08-2020.11) and the United Kingdom's Natural Environment Research Council (NE/S002847/1)



## References

- 245 Ali, H., Fowler, H.J., Vanniere, B. and Roberts, M.J. Fewer, but more intense, future Tropical Storms over the Ganges and Mekong basins. *Geophysical Research Letters*, 50(17), <https://dx.doi.org/10.5258/SOTON/WP00647>, 2023.
- Arnell, N.W. and Gosling, S.N., The impacts of climate change on river flow regimes at the global scale. *Journal of Hydrology*, 486, pp.351-364. <https://doi.org/10.1016/j.jhydrol.2013.02.010>, 2013.
- Bloemendaal, N., de Moel, H., Martinez, A.B., Muis, S., Haigh, I.D., van der Wiel, K., Haarsma, R.J., Ward, P.J., Roberts, M.J., Dullaart, J.C. and Aerts, J.C., A globally consistent local-scale assessment of future tropical cyclone risk. *Science advances*, 8(17), <https://doi.org/10.1126/sciadv.abm8438>, 2022.
- 250 Bui, T.T., Kantoush, S., Kawamura, A., Du, T.L., Bui, N.T., Capell, R., Nguyen, N.T., Du Bui, D., Saber, M., Tetsuya, S. and Lee, H., 2023. Reservoir operation impacts on streamflow and sediment dynamics in the transboundary river basin, Vietnam. *Hydrological Processes*, 37(9), <https://doi.org/10.1002/hyp.14994>, 2023.
- 255 Burkey J. 2021Mann-Kendall Tau-b with Sen's Method (enhanced) <https://www.mathworks.com/matlabcentral/fileexchange/11190-mann-kendall-tau-b-with-sen-s-method-enhanced>, MATLAB Central File Exchange. Retrieved: November 2021.
- Darby, S., Hackney, C., Leyland, J. et al. Fluvial sediment supply to a mega-delta reduced by shifting tropical-cyclone activity. *Nature* 539, 276–279. <https://doi.org/10.1038/nature19809>, 2016.
- 260 Devitt, L., Neal, J., Coxon, G., Savage, J. and Wagener, T., Flood hazard potential reveals global floodplain settlement patterns. *Nature Communications*, 14(1), p.2801. <https://doi.org/10.1038/s41467-023-38297-9>, 2023
- Di Baldassarre, G., Kooy, M., Kemerink, J.S. and Brandimarte, L., Towards understanding the dynamic behaviour of floodplains as human-water systems. *Hydrology and Earth System Sciences*, 17(8), pp.3235-3244. <https://doi.org/10.5194/hess-17-3235-2013>, 2013.
- 265 Du, T.L., Lee, H., Bui, D.D., Arheimer, B., Li, H.Y., Olsson, J., Darby, S.E., Sheffield, J., Kim, D. and Hwang, E.. Streamflow prediction in “geopolitically ungauged” basins using satellite observations and regionalization at subcontinental scale. *Journal of Hydrology*, 588, p.125016. <https://doi.org/10.1016/j.jhydrol.2020.125016>, 2020.
- Du, T.L., Lee, H., Bui, D.D., Graham, L.P., Darby, S.D., Pechlivanidis, I.G., Leyland, J., Biswas, N.K., Choi, G., Batelaan, O. and Bui, T.T. Streamflow prediction in highly regulated, transboundary watersheds using multi-basin modeling and remote sensing imagery. *Water resources research*, 58(3). <https://doi.org/10.1029/2021WR031191>, 2022.
- 270 Englehart, P.J. & Douglas, A.V. The role of eastern North Pacific tropical storms in the rainfall climatology of western Mexico. *Int. J. Climatol.* 21, 1357–1370. <https://doi.org/10.1002/joc.637>, 2001.
- Franco-Díaz, A., Klingaman, N. P., Vidale, P. L., Guo, L., & Demory, M. E. The contribution of tropical cyclones to the atmospheric branch of middle America's hydrological cycle using observed and reanalysis tracks. *Climate Dynamics*, 53(9), 6145–6158. <https://doi.org/10.1007/s00382-019-04920-z>, 2019.



- Gebrechorkos, S., Leyland, J., Slater, L. *et al.* A high-resolution daily global dataset of statistically downscaled CMIP6 models for climate impact analyses. *Sci Data* **10**, 611. <https://doi.org/10.1038/s41597-023-02528-x>, 2023.
- Gupta, S., Indu J., Pushpendra J., and Murari L., Impact of Climate Change on Tropical Cyclones Frequency and Intensity on Indian Coasts. In: Rao, P., Rao, K., Kubo, S. (eds) Proceedings of International Conference on Remote Sensing for  
280 Disaster Management. Springer Series in Geomechanics and Geoengineering. p. 359. Springer, Cham.  
[https://doi.org/10.1007/978-3-319-77276-9\\_32](https://doi.org/10.1007/978-3-319-77276-9_32), 2019.
- Hersbach, H., Bell, B., Berrisford, P., Hirahara, S., Horányi, A., Muñoz-Sabater, J., Nicolas, J., Peubey, C., Radu, R., Schepers, D. and Simmons, A. The ERA5 global reanalysis. *Quarterly Journal of the Royal Meteorological Society*, 146(730), pp.1999-2049. <https://doi.org/10.1002/qj.3803>, 2020.
- 285 Hirabayashi, Y., Mahendran, R., Koirala, S. *et al.* Global flood risk under climate change. *Nature Clim Change* **3**, 816–821.  
<https://doi.org/10.1038/nclimate1911>, 2013
- IPCC (The Intergovernmental Panel on Climate Change). Special Report. Global Warming of 1.5C.  
[www.ipcc.ch/report/sr15/](http://www.ipcc.ch/report/sr15/), 2018
- Jing, R., Heft-Neal, S., Chavas, D.R., Griswold, M., Wang, Z., Clark-Ginsberg, A., Guha-Sapir, D., Bendavid, E. and  
290 Wagner, Z., Global population profile of tropical cyclone exposure from 2002 to 2019. *Nature*, 626(7999), pp.549-554.  
<https://doi.org/10.1038/s41586-023-06963-z>, 2024.
- Jongman, B., Winsemius, H.C., Aerts, J.C., Coughlan de Perez, E., Van Aalst, M.K., Kron, W. and Ward, P.J., Declining vulnerability to river floods and the global benefits of adaptation, *Proc. Natl. Acad. Sci. U.S.A.* **112** (18) E2271-E2280,  
<https://doi.org/10.1073/pnas.1414439112>, 2015.
- 295 Knapp, K. R., M. C. Kruk, D. H. Levinson, H. J. Diamond, and C. J. Neumann,. The International Best Track Archive for Climate Stewardship (IBTrACS): Unifying tropical cyclone best track data. *Bulletin of the American Meteorological Society*, **91**, 363-376. <https://doi.org/10.1175/2009BAMS2755.1>, 2010.
- Knutson, T. R., McBride, J. L., Chan, J., Emanuel, K., Holland, G., Landsea, C., *et al.*, Tropical cyclones and climate change. *Nature Geoscience*, **3**(3), 157–163. <https://doi.org/10.1038/ngeo779>, 2010.
- 300 Knutson, T.R., Sirutis, J.J., Zhao, M., Tuleya, R.E., Bender, M., Vecchi, G.A., Villarini, G. and Chavas, D., Global projections of intense tropical cyclone activity for the late twenty-first century from dynamical downscaling of CMIP5/RCP4. 5 scenarios. *Journal of Climate*, **28**(18), pp.7203-7224. <https://doi.org/10.1175/JCLI-D-15-0129.1>, 2015.
- Kundzewicz, Z.W., Kanae, S., Seneviratne, S.I., Handmer, J., Nicholls, N., Peduzzi, P., Mechler, R., Bouwer, L.M., Arnell, N., Mach, K. and Muir-Wood, R., Flood risk and climate change: global and regional perspectives. *Hydrological Sciences Journal*, **59**(1), pp.1-28. <https://doi.org/10.1080/02626667.2013.857411>, 2014.
- 305 Lindström, G., Pers, C., Rosberg, J., Strömqvist, J. & Arheimer, B. Development and testing of the HYPE (Hydrological Predictions for the Environment) water quality model for different spatial scales. *Hydrology Research* **41.3–4**, 295-319. <https://doi.org/10.2166/nh.2010.007>, 2010.



- Macalalad, R.V., Badilla, R.A., Cabrera, O.C. and Bagtasa, G., 2021. Hydrological response of the Pampanga River basin in the Philippines to intense tropical cyclone rainfall. *Journal of Hydrometeorology*, 22(4), pp.781-794.  
<https://doi.org/10.1175/JHM-D-20-0184.1>
- 310
- Maher, N., Wills, R. C. J., DiNezio, P., Klavans, J., Milinski, S., Sanchez, S. C., Stevenson, S., Stuecker, M. F., and Wu, X.: The future of the El Niño–Southern Oscillation: using large ensembles to illuminate time-varying responses and inter-model differences, *Earth Syst. Dynam.*, 14, 413–431, <https://doi.org/10.5194/esd-14-413-2023>, 2023.
- 315
- Mann, H.B. Non-parametric tests against trend. *Econometrica* 13 p. 245–259. <https://doi.org/10.2307/1907187>, 1945.
- Murakami, H., Wang, B., Li, T. and Kitoh, A., Projected increase in tropical cyclones near Hawaii. *Nature Climate Change*, 3(8), pp.749-754. <https://doi.org/10.1038/nclimate1890>, 2013
- Polade, S.D., Gershunov, A., Cayan, D.R., Dettinger, M.D. and Pierce, D.W., Precipitation in a warming world: Assessing projected hydro-climate changes in California and other Mediterranean climate regions. *Scientific reports*, 7(1), p.10783.  
<https://doi.org/10.1038/s41598-017-11285-y>, 2017.
- 320
- Rentschler, J., Avner, P., Marconcini, M., Su, R., Strano, E., Vousdoukas, M. and Hallegatte, S., Global evidence of rapid urban growth in flood zones since 1985. *Nature*, 622(7981), pp.87-92. <https://doi.org/10.1038/s41586-023-06468-9>, 2023.
- Rentschler, J., Salhab, M. & Jafino, B.A. Flood exposure and poverty in 188 countries. *Nat Commun* 13, 3527.  
<https://doi.org/10.1038/s41467-022-30727-4>, 2022.
- 325
- Roberts, M. J., Baker, A., Blockley, E. W., Calvert, D., Coward, A., Hewitt, H. T., Jackson, L. C., Kuhlbrodt, T., Mathiot, P., Roberts, C. D., Schiemann, R., Seddon, J., Vannière, B., and Vidale, P. L. Description of the resolution hierarchy of the global coupled HadGEM3-GC3.1 model as used in CMIP6 HighResMIP experiments, *Geosci. Model Dev.*, 12, 4999–5028, <https://doi.org/10.5194/gmd-12-4999-2019>, 2019.
- 330
- Roberts, M. J., Camp, J., Seddon, J., Vidale, P. L., Hodges, K., Vannière, B., et al., Projected future changes in tropical cyclones using the CMIP6 HighResMIP multimodel ensemble. *Geophysical Research Letters*, 47(14): e2020GL088662. <https://doi.org/10.1029/2020gl088662>, 2020.
- Rodgers, E.B., Adler, R.F. and Pierce, H.F. Contribution of tropical cyclones to the North Pacific climatological rainfall as observed from satellites. *Journal of Applied Meteorology and Climatology*, 39(10), pp.1658-1678.  
[https://doi.org/10.1175/1520-0450\(2000\)039%3C1658:COTCTT%3E2.0.CO;2](https://doi.org/10.1175/1520-0450(2000)039%3C1658:COTCTT%3E2.0.CO;2), 2000.
- 335
- Sun, N., Wigmosta, M.S., Judi, D., Yang, Z., Xiao, Z. and Wang, T., 2021. Climatological analysis of tropical cyclone impacts on hydrological extremes in the Mid-Atlantic region of the United States. *Environmental research letters*, 16(12), p.124009. <https://doi.org/10.1088/1748-9326/ac2d6a>
- WorldPop ([www.worldpop.org](http://www.worldpop.org) – School of Geography and Environmental Science, University of Southampton; Department of Geography and Geosciences, University of Louisville; Département de Géographie, Université de Namur) and Center for International Earth Science Information Network (CIESIN), Columbia University. Global High Resolution
- 340

<https://doi.org/10.5194/egusphere-2025-3506>

Preprint. Discussion started: 8 August 2025

© Author(s) 2025. CC BY 4.0 License.



Population Denominators Project – Funded by The Bill and Melinda Gates Foundation (OPP1134076). Retrieved: March 2023.